



THE FINITE ELEMENT THERMAL ANALYSIS OF GRINDING PROCESSES BY ADINA

M. Mahdi and Liangchi Zhang

Centre for Advanced Material Technology, Department of Mechanical and Mechatronic Engineering,
The University of Sydney, NSW 2006, Australia

Abstract—Most grinding problems cannot be solved analytically, therefore extensive numerical solutions are required by using appropriate numerical techniques such as the finite element method (FEM). In this study, the well-known finite element software, ADINA, was used to predict the phase transformation of a workpiece subjected to surface grinding. The process was considered to be two-dimensional and the properties of the workpiece material were temperature dependent. To gain practically acceptable results, the induced temperature field and the associated phase transformation were analysed by different element meshes. Some efficient solution strategies were proposed to obtain reliable predictions for different grinding conditions and workmaterial properties. The user coding facilities of the code were used to achieve the above performances.

NOTATION

c	specific heat capacity per unit volume of ground components
D	non-dimensional martensite depth (d/l)
d	depth of martensite
H	non-dimensional heat transfer coefficient ($2\alpha h/kv$)
h	heat transfer coefficient of coolant
k	thermal conductivity of ground components
l	half length of grinding zone, see Fig. 1
l_p	relative peak location of a heat flux (x_p/l), see Fig. 1
q	heat flux per unit grinding width
\bar{q}	average heat flux
q_p	peak value of the heat flux
q_c	heat transferred by convection (hT), see Fig. 1
Pe	Peclet number ($vl/2\alpha$)
r	$(x^2 + z^2)^{1/2}$
T	temperature rise ($T_w - T_\infty$), with respect to ambient temperature
T	non-dimensional temperature ($\pi kvT/2\alpha\bar{q}$)
T_*	workmaterial temperature
T_∞	ambient temperature
t	time
\bar{t}	non-dimensional time ($v^2 t/2\alpha_\infty$)
v	moving speed of the heat source, equal to the table speed set of the grinding machine, see Fig. 1
X, X'	non-dimensional horizontal coordinate, i.e. x/l and x'/l , respectively
x, z	coordinates of the stationary reference frame, see Fig. 1
x', z'	coordinates of the moving reference frame, see Fig. 1
x_p	horizontal coordinate of peak heat flux location, see Fig. 1
α	thermal diffusivity
∞	at room temperature

It is well-known that such temperature rise plays an important role in the formation of residual stresses in a ground component which is a key factor of surface integrity.

A main cause of residual stresses is the phase transformation of the surface material, characterized by critical grinding temperature histories. Fundamentally, as summarised by Ref. [1], there are four problems in the thermal analysis of phase transformation associated with grinding: (1) the strength and distribution of the heat source generated, which relates to the material removal mechanisms of grinding; (2) the convection of cooling media, which reflects the effect of coolant; (3) the thermal properties of the workmaterial; and (4) the moving speed of the heat source.

Most of the relevant studies of grinding temperature (e.g. Refs [2-7]) were based on Jaeger's model [8] proposed in the 1940s, where a heat source of constant strength moving on the surface of a half-plane was considered. Isenberg and Malkin [9] considered the effects of variable thermal properties of workmaterial and presented a set of numerical results of grinding temperature induced by a moving band source of constant strength. However, the dependence of thermal properties on temperature was assumed to be linear. Li and Chen [10] developed an improved model to investigate grinding temperature and residual stresses due to both mechanical and thermal factors, but the workmaterial properties considered were temperature-independent and the moving heat sources were of constant strength. Recently, Zhang *et al.* reviewed the previous work [11], discussed the relevant problem of moving heat sources of constant and triangular input profiles and studied their effects in terms of grinding conditions [1, 12]. They analysed grinding temperature using

1. INTRODUCTION

Grinding requires an extremely high energy input per unit volume of material removal compared with other machining processes, and almost all of the energy is converted to heat which is concentrated in the grinding zone. This usually leads to an elevated temperature rise in both the wheel and workpiece.

ADINA and correlated it with grinding conditions and phase transformation. However, the comprehensive effect of the input heat flux profile with temperature dependent material properties has not been investigated so far.

With the aid of the ADINA code, this paper discusses the phase transformation of an alloy steel with temperature-dependent properties. Particular attention has been paid to the effects of Peclet number and the strength of profile of heat source on martensite depth.

2. PROBLEM MODELLING WITH ADINA

2.1. Problem description

As in Ref. [11], a surface grinding process is assumed to be two-dimensional. The heat source profile is triangular, moving along the positive direction of the x axis on the workpiece surface, as shown in Fig. 1. For a stationary frame of reference (x oz), the general governing eqn [13] is

$$\frac{\partial}{\partial x} \left(k \frac{\partial T}{\partial x} \right) + \frac{\partial}{\partial z} \left(k \frac{\partial T}{\partial z} \right) = c \frac{\partial T}{\partial t} \quad (1)$$

where $T = T_w - T_\infty$ is the temperature rise in the workmaterial relative to the ambient temperature T_∞ , c is the specific heat capacity per unit volume of the workmaterial, t is time, k is the thermal conductivity of workmaterial and x and z are the horizontal and vertical coordinates, see Fig. 1. If the frame of reference moves with a constant speed v , which is equal to the table speed set of the grinding machine, eqn (1) becomes

$$\frac{\partial}{\partial x'} \left(k \frac{\partial T}{\partial x'} \right) + \frac{\partial}{\partial z} \left(k \frac{\partial T}{\partial z} \right) + \frac{\partial}{\partial x'} (cvT) = 0, \quad (2)$$

where x' is the horizontal coordinate of the moving reference frame.

For materials with constant thermal properties eqns (1) and (2) could be simplified to

$$\frac{\partial^2 T}{\partial x^2} + \frac{\partial^2 T}{\partial z^2} = \frac{1}{\alpha} \frac{\partial T}{\partial t}, \quad (3)$$

and

$$\frac{\partial^2 T}{\partial x'^2} + \frac{\partial^2 T}{\partial z^2} + \frac{v}{\alpha} \frac{\partial T}{\partial x'} = 0, \quad (4)$$

respectively, where α is the thermal diffusivity of the workmaterial.

A general heat transfer model is available in ADINA [14]. The model which may be used for studying steady and transient heat transfer problems accounts for many important non-linear characteristics of thermal properties of a workmaterial. However, due to the nature of the moving boundary conditions associated with grinding conditions the

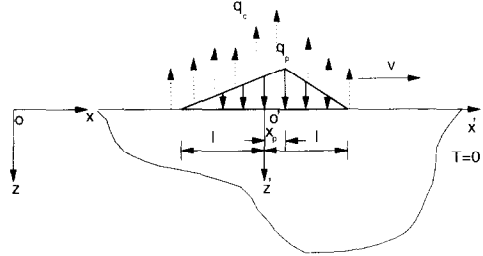


Fig. 1. A model for the thermal analysis of surface grinding.

use of the model requires great user-expertise and the computational cost can be very high. To overcome this, the flexibility of ADINA in providing users with the options of constructing a user-model is employed to develop a material model suitable for the solutions of eqns (1)–(4). In the following sections the material models along with their implementation into ADINA are presented.

In this study, the boundary conditions associated with the heat flux input and heat transfer due to convection could be described as

$$\frac{\partial T}{\partial z} = \begin{cases} \frac{1}{k} (-q(x') + hT), & |x'| \leq l, z = 0 \\ \frac{1}{k} (hT), & |x'| \leq l, z = 0 \end{cases}, \quad (5.1)$$

and

$$T, \frac{\partial T}{\partial r} \rightarrow 0, \quad \text{when } r \rightarrow \infty \quad (5.2)$$

where

$$q(x') = \begin{cases} \frac{q_p}{x_p + 1} (x' + 1), & -1 \leq x' \leq x_p \\ \frac{q_p}{1 - x_p} (1 - x'), & x_p \leq x' \leq 1 \end{cases}, \quad (5.3)$$

$r = (x^2 + z^2)^{1/2}$, x_p is the apex coordinate of the heat flux relative to the moving frame, h the convection heat transfer coefficient of the coolant and q_p the peak heat flux input, see Fig. 1.

2.2. Material model

The main advantage of the material model developed below is its applicability in terms of solution stability and computational cost. The model can be used for general moving boundary conditions associated with moving heat sources. As stated in Section 1, the material model is defined by a user-supplied code written in Fortran and inserted into CUSER2 and CUSERH. It is then compiled and linked to other object files for program execution. This model expresses grinding conditions and thermal properties in terms of materials parameters of either temperature-independent or temperature-dependent properties.

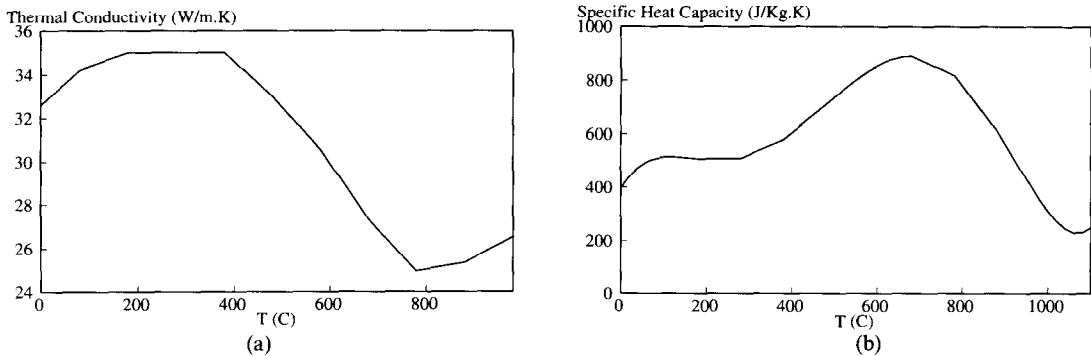


Fig. 2. Thermal properties of EN23 steel, (a) thermal conductivity, (b) specific heat capacity.

2.2.1. Materials with temperature-independent properties. To model the two-dimensional steady state grinding process, the relevant governing equation and boundary conditions solved by ADINA [14] are

$$\frac{\partial}{\partial x'} K(x') + K(x') \frac{\partial^2 T}{\partial x'^2} + K(x') \frac{\partial^2 T}{\partial z'^2} = 0, \quad (6)$$

and

$$\frac{\partial T}{\partial z} = \frac{1}{K} (-Q(x')), \quad z = 0, \quad (7)$$

respectively, where $K(x')$ is the thermal conductivity and $Q(x')$ the input heat flux at x' . As compared with eqn (4), eqn (6) may yield the same temperature solution if

$$\frac{1}{cv} \left(\frac{dK}{dx'} \right) = \frac{K}{k}. \quad (8)$$

Integrating eqn (8) yields

$$K = k_0 \exp\left(\frac{vx'}{\alpha}\right), \quad (9)$$

where k_0 is a non-zero integration constant. Substituting eqn (9) into eqn (6) yields

$$k_0 \exp\left(\frac{vx'}{\alpha}\right) \left(\frac{\partial^2 T}{\partial x'^2} + \frac{\partial^2 T}{\partial z'^2} + \frac{v}{\alpha} \frac{\partial T}{\partial x'} \right) = 0. \quad (10)$$

Since the first term of eqn (10) is non-vanishing, the second term should be zero which precisely yields the same equation as eqn (4). To obtain

the same temperature gradients as eqn (5), $Q(x')$ should be

$$Q(x') = \begin{cases} \frac{K}{k} (-q(x') + hT), & |x'| \leq l, z = 0 \\ \frac{K}{k} (hT), & |x'| > l, z = 0. \end{cases} \quad (11)$$

Correspondingly, the following relevant boundary conditions:

$$\begin{cases} \frac{\partial T}{\partial z} = \begin{cases} \frac{k_0}{k} (-q(x') + ht) \exp\left(\frac{vx'}{\alpha}\right), & |x'| \leq l, z = 0 \\ \frac{k_0}{k} (ht) \exp\left(\frac{vx'}{\alpha}\right), & |x'| > l, z = 0 \end{cases} \\ T, \frac{\partial T}{\partial r} \rightarrow 0, \quad \text{when } r \rightarrow \infty \end{cases} \quad (12)$$

should be used to replace eqn (5) when ADINA is used to solve for the grinding problem with a moving heat source.

2.2.2. Materials with temperature-dependent properties. For materials with temperature-dependent thermal properties [15, 16] illustrated in Fig. 2 and Table 1, it is generally impossible to transform eqn (2) to an equivalent steady state equation. Thus a transient model based on eqn (1) needs to be developed. This modelling requires the simulation of heat source movement over a stationary workmaterial surface ($z = 0$). Therefore the control volume needs to be attached to the fixed frame of reference (xoz) as shown in Fig. 1. Compared with the above steady state solutions strategy, the transient model needs much larger memory space and computational time.

Table 1. The composition and phase change properties of EN23 steel

C	Si	Mn	Composition (% weight) Cr	Mo	Ni	Critical cooling time between 1029 K and 773 K	Austenizing temperature (K)
0.32	0.25	0.55	0.71	0.06	3.41	<1.6	1123

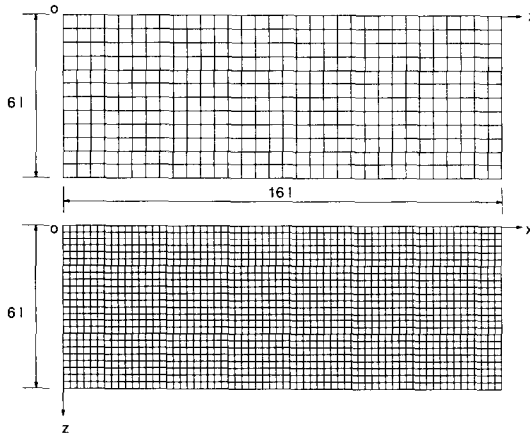


Fig. 3. Finite elements meshes, (a) with 32×12 nine-noded elements, (b) with 64×24 nine-noded elements.

2.3. Control volume determination

Although the problems considered are semi-infinite, a reasonable defined control volume must be used to model the associated open boundary conditions at ($x = -\infty, z = \infty$) for the finite element method. A typical value of a grinding zone length of 2 mm is used throughout the calculations. To propose a proper dimension of such a control volume (and thus the accurate modelling of the open boundary conditions associated with the semi-infinite domain) relevant temperature solutions are required for comparison. However, there are no analytical solutions available for the temperature-dependent thermal properties. Therefore, the solutions associated with constant material properties are used to estimate the most adequate control volume for the boundary conditions (5). The proposed control volume has been checked, in the most important region $2 < X' < 5$, against the relevant analytical solutions [8] and shows that temperature would become negligible as $X' > 4$. Hence the right boundaries of the control volume should be beyond $X' = 4$. The depth of the control volume required for this study is $Z' = 6$ to approximate the isolated conditions of eqn (5) with an estimated temperature gradient error of 2%.

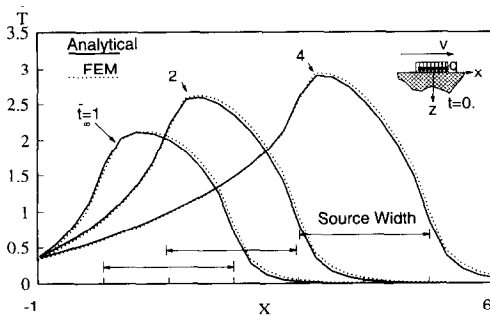


Fig. 4. Transient temperature profiles with $Pe_\infty = 1$, $Z = 0$ and $H_\infty = 0$.

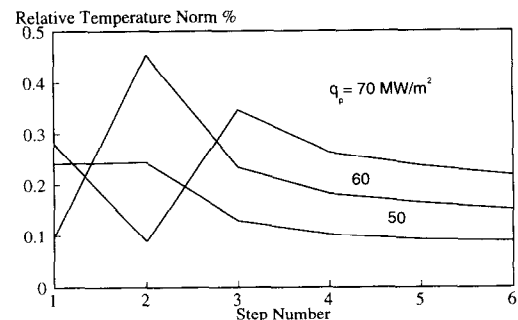


Fig. 5. Typical converging curves with $l_p = 0.25$ and $Pe_\infty = 1$.

2.4. Finite element modelling

For the alloy steel (En23) investigated here, the phase transformation is induced by austenizing and quenching characterized by critical temperature histories [16]. For a realistic solution of the problem, the variations of thermal properties of workmaterial need to be considered. Thus the temperature dependent material model should be used to relate thermal properties with temperature.

To obtain the induced phase transformation, it is necessary to determine temperature history within the workmaterial due to the moving heat source. This is accomplished through a number of finite movements of the heat source from a specified initial position to a final position. Therefore, the continuum representing the stationary control volume is divided by

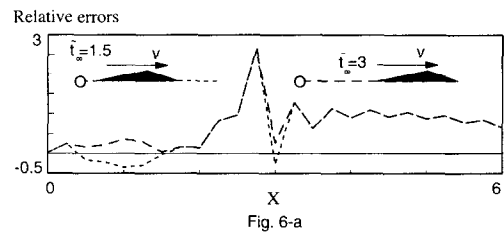


Fig. 6-a

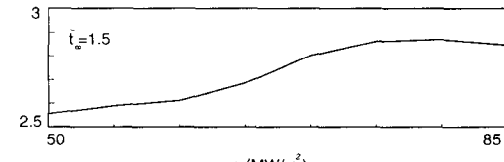


Fig. 6-b

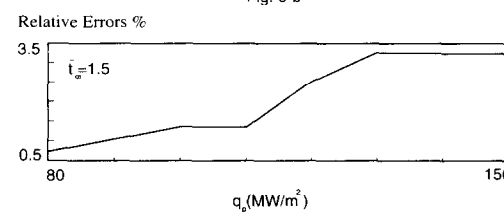


Fig. 6-c

Fig. 6. Relative errors due to mesh refinement ($H_\infty = 0$), (a) $Pe_\infty = 1$ and $q_p = 50 \text{ MW m}^{-2}$, (b) $Pe_\infty = 1$, (c) $Pe_\infty = 4$.

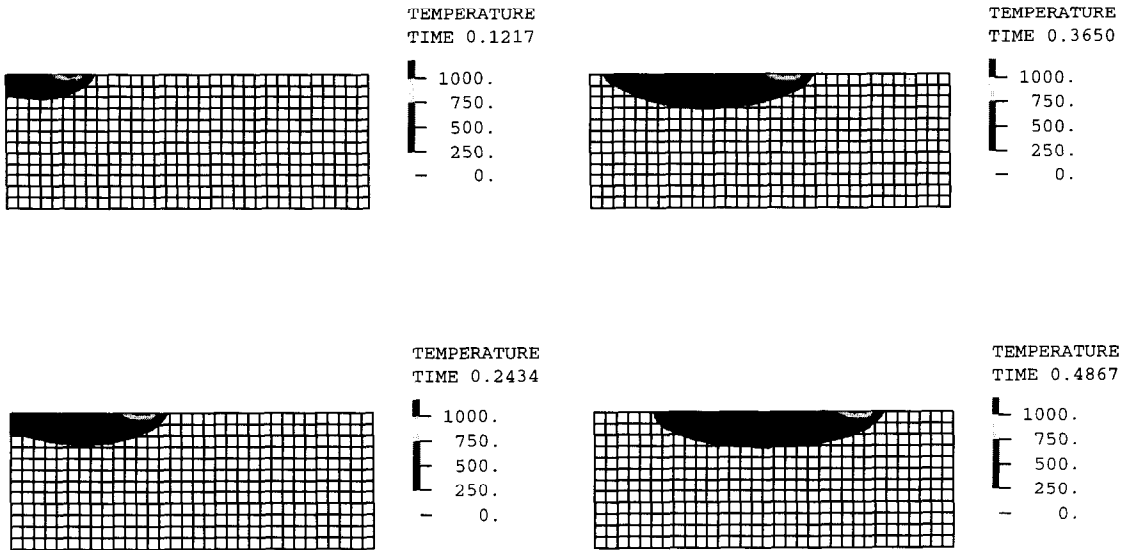


Fig. 7. A transient temperature field with $q_p = 85 \text{ MW m}^{-2}$, $H_\infty = 0$, $l_p = 0.25$ and $Pe_\infty = 1$.

nine-noded isoparametric quadratic finite elements as shown in Fig. 3. The size of the stationary control volume is composed of 384 elements and 1625 nodes for the coarse mesh and 1536 elements and 6321 nodes for the fine one. To ensure an adequate and stable transient grinding temperature simulation, the size of the time step, the locations of the initial and the final positions of the heat source and the time integration scheme (backward) are chosen to approximate the movement of the heat source over the interval $0 < X < 12$.

For obtaining a reliable temperature field, an accuracy criterion is required to predict convergence. There are several options for estimating the solution errors. For the cases of constant material properties, the solution errors are determined based on the comparison with a set of analytical solutions available [8]. A typical transient FEM solution, with a mesh shown in Fig. 3-9, is compared with the

relevant analytical solution and shows good agreement in terms of stability and accuracy (see Fig. 4). However, the cases of temperature-dependent properties of workmaterials need special strategies to estimate the convergence errors. Usually, the convergence rates increase (with a limit) as relative iteration errors and mesh size decrease. Thus a smaller relative iteration error and mesh size may imply a more accurate solution. The limiting maximum tolerance of the relative iteration error [14] throughout this study is bounded by 0.5%. The iteration error history associated with typical grinding conditions is monitored and found to be asymptotic as illustrated in Fig. 5. Moreover, the iteration error increases as q_p increases. This means that a high heat flux yields a much higher temperature rise and hence more complicated dependence of workmaterial properties on temperature. To decrease the iteration error, uniform finer elements are used and the solution accuracy of

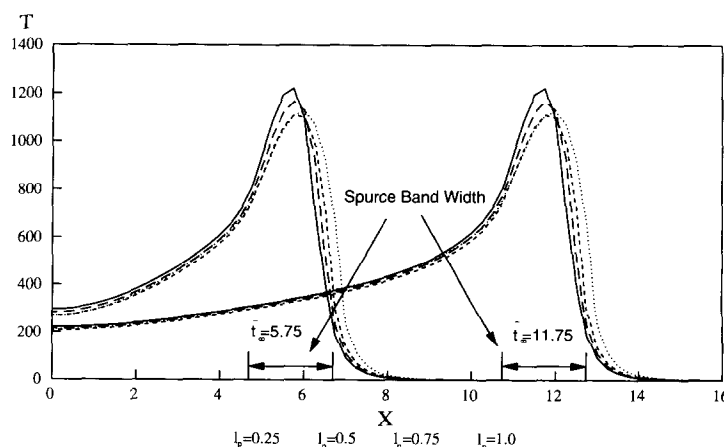


Fig. 8. A transient surface temperature with, $q_p = 85 \text{ MW m}^{-2}$, $H_\infty = 0$ and $Pe_\infty = 1$.

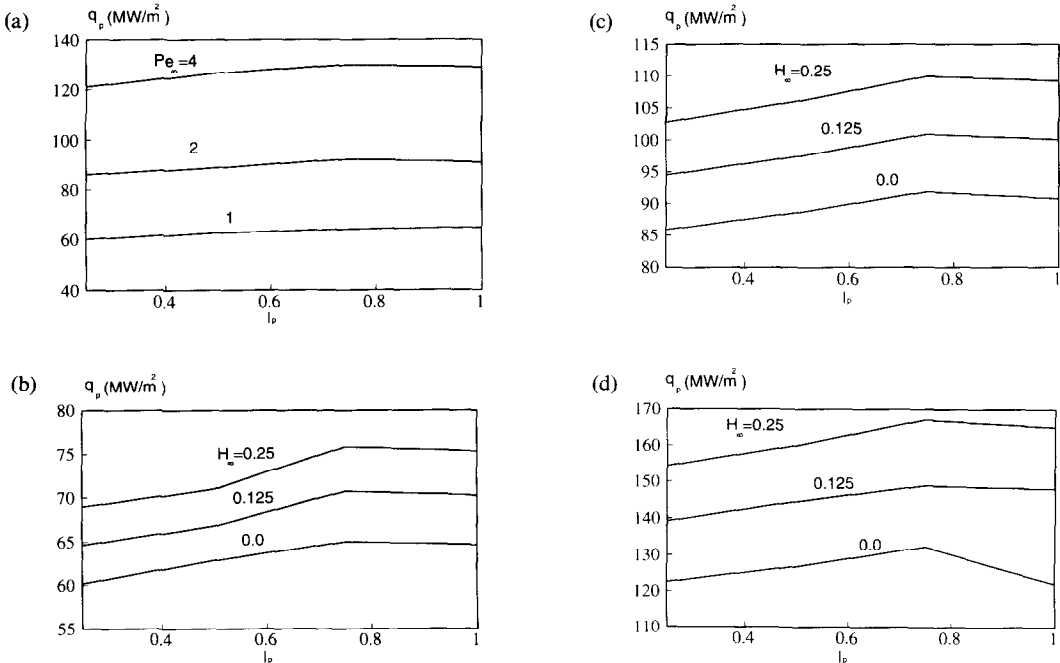


Fig. 9. Critical curves for the onset of martensite transformation, (a) $H_\infty = 0$, (b) $Pe_\infty = 1$, (c) $Pe_\infty = 2$, (d) $Pe_\infty = 4$.

the non-linear analysis is estimated by comparing the variation of surface temperature with decreasing mesh size. A typical relative error due to mesh refinement is checked in the most important region ($-1 < X' < 0, Z = 0$), illustrated in Fig. 6. The maximum error is 3.5%, which is very acceptable in most engineering applications.

3. RESULTS AND DISCUSSION

3.1. Temperature

The heat generated within the grinding zone raises the grinding temperature. As the heat source moves on the surface, the associated temperature field within the continuum also moves, thereby causing a

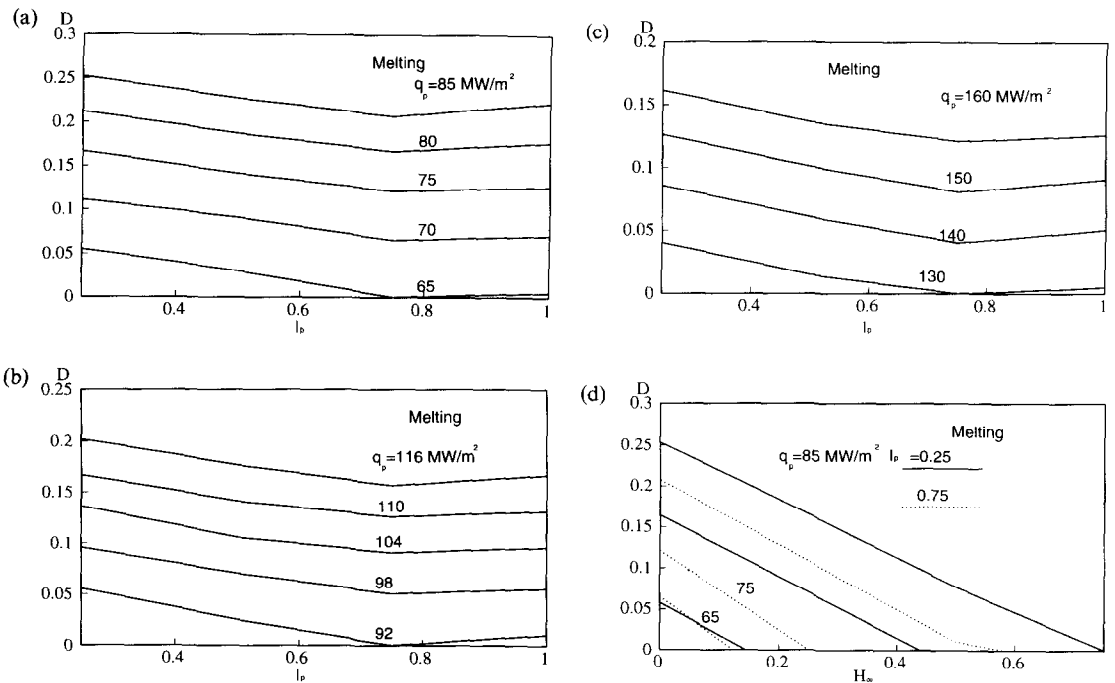


Fig. 10. Variation of martensite depth with q_p , (a) $Pe_\infty = 1$, (b) $Pe_\infty = 2$, (c) $Pe_\infty = 4$, (d) $l_p = 0.25$ and 0.75 .

temperature change in the workmaterial as shown in Fig. 7. Clearly, the developed transient temperature field approaches its steady state after few movement steps of the input heat flux over the workpiece surface. Moreover, the implicit (backward) time integration scheme used results in a stable transient temperature solution. Similar to [12], the effect of l_p on surface temperature has been investigated for $P_e = 1$ (Fig. 8) and shows that highest surface temperature occurs when $l_p = 0.25$. It should be noted that the maximum surface decreases as l_p increases when $l_p < 0.75$. The least maximum temperature in terms of l_p is at $l_p = 0.75$.

3.2. Critical grinding conditions

The critical grinding conditions are reached when the onset of martensite transformation is observed. Typical results are shown in Fig. 9. The effects of l_p , H_∞ and P_e on phase transformation are clearly demonstrated. With a higher P_e , i.e. a higher table speed, the onset of martensite needs a higher heat input with a specific H_∞ value. This means that increasing v yields much heat diffusion in the work material and hence less grinding temperature rise. The cooling effect shows that more heat flux input is required as H_∞ increases. On the other hand, for a smaller l_p , i.e. the peak of the heat flux being closer to the centre of the grinding zone, the onset of martensite needs a lower heat input. Moreover the least significant cases are associated with $l_p = 0.75$ which are slightly different from that with $l_p = 1.0$ in the case of constant properties [12]. This implies that the critical conditions for components with temperature-dependent properties may not change much with the type of grinding operation in a certain range, if all the other grinding parameters are the same.

3.3. Predicted martensite depths

A parametric study is conducted to investigate the effects of l_p , q_p , and H_∞ when $P_e = 1$ is given. Figure 10 shows (with melting limits) that a higher q_p yields a higher martensite depth. It is similar to the results of materials with temperature-independent properties. On the other hand, changes of martensite depths are more significant when $l_p = 0.25$ and 1. The effects of H_∞ on the extent of martensite, as illustrated in Fig. 10d, shows that martensite depth decreases monotonically as H_∞ increases. This means, as in Ref. [1], coolant effect makes the critical temperature zone thinner. Compared with the results of temperature-independent materials, the dependence of material properties on temperature alters the formation of phase transformation. For the particular material studied, this dependence diminishes the difference of phase transformation in the range of $0.75 < l_p < 1$ when the type of grinding operation is changed. The development of martensite extent is investigated for the most critical grinding conditions ($P_e = 1$ and $H_\infty = 0$). The results (Fig. 11) show

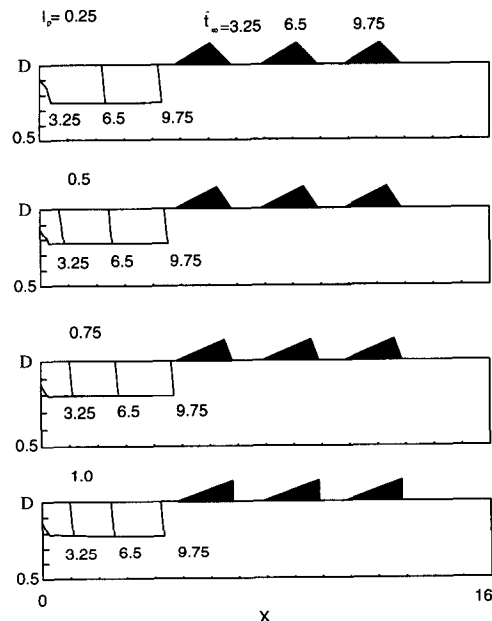


Fig. 11. Martensite transformation with $q_p = 85 \text{ MW m}^{-2}$, $l_p = 0.25$ and $H_\infty = 0$.

that a larger l_p would cause earlier martensite transformation.

4. CONCLUSIONS

A useful finite element material model has been developed and employed to investigate the correlation between the critical grinding conditions and the phase transformation. It concludes that:

(1) To simulate the moving heat sources associated with grinding by ADINA, a user supplied material model (CUSER2 and CUSERH) needs to be built up. For problems with constant workmaterial properties, the steady state model provided by ADINA can be employed indirectly. For those with temperature-dependent properties, a transient model must be used at a cost of increasing memory storage and computing time.

(2) $l_p = 0.25$ and 1 are the most critical grinding conditions of this particular temperature-dependent workmaterial properties since they yield a higher martensite depth. Much attention should be paid for the dependence of workmaterial properties on temperature for different grinding processes such as down- and up-grinding operations in the range of $0 < l_p < 0.75$.

Acknowledgment—The financial support from ARC Small Grant to the present study is appreciated. The ADINA code was used for all the calculations.

REFERENCES

1. L. C. Zhang and M. Mahdi, Applied mechanics in grinding, part IV: grinding induced phase transformation. *Int. J. Mach. Tools Manuf.*, in press.
2. J. O. Outwater and M. C. Shaw, Surface temperature in grinding. *Trans. ASME* **74**, 73–86 (1952).

3. R. S. Hahn, The relation between grinding conditions and thermal damage in the workpiece. *Trans ASME* **78**, 807–812 (1956).
4. N. R. Des Ruisseaux and R. D. Zerkle, Thermal analysis of grinding process. *J. Engng Ind.* **92**, 428–434 (1970).
5. S. Makkine and R. B. Andorson, Thermal aspects of grinding. Part 1: energy partition. *J. Engng Ind.* **96**, 1177–1183 (1974).
6. S. Makkine, Thermal aspects of grinding. Part 2: surface temperature and workpiece burn. *J. Engng Ind.* **96**, 1183–1191 (1974).
7. N. R. Des Ruisseaux and R. D. Zerkle, Temperature in semi-infinite and cylindrical bodies subjected to moving heat sources and surface cooling. *J. Heat Transfer Trans. ASME* 456–464 (1970).
8. J. Jaeger, Moving sources of heat and the temperature at sliding contacts. *J. Proc. R. Soc. N.S.W.* **76**, Part 3 (1942).
9. J. Isenberg and S. Malkin, Effects of variable thermal properties on moving-band-source temperatures. *J. Engng Ind. Trans. ASME* 1074–1078 (1975).
10. Y. Y. Li and Y. Chen, Simulation of surface grinding. *J. Engng Mater. Technol. Trans. ASME* **111**, 46–53 (1989).
11. L. C. Zhang, T. Suto, H. Noguchi and T. Waid, An overview of applied mechanics. *Mfg Rev.* **5**(4), 261–273 (1992).
12. M. Mahdi and L. C. Zhang, Correlation between grinding conditions and phase transformation of an alloy steel. *Proc. Advanced Computational Methods in Heat Transfer III*, pp. 193–200 (1994).
13. H. S. Carslaw and J. C. Jaeger, *Conduction of Heat in Solids* (2nd Edn). Oxford University Press, Great Britain (1965).
14. ADINA R & D, Theory and modelling guide. Report ARD 92-5, ADINA R & D (1992).
15. British Iron and Steel Research Association, *The Mechanical and Physical Properties of the British Standard on Steels*, Vol. 2. Pergamon Press, Oxford (1969).
16. M. Atkin, *Atlas of Continuous Cooling Transformation diagrams for Engineering Steels*. Market Promotion Department, British Steel Corporation, BBC Billet, Bar and Rod Products, Sheffield, UK (1977).